J|A|C|S
ARTICLES
Published on Web 10/17/2003

Impressive Structural Diversity and Polymorphism in the Modular Compounds ABi_3Q_5 (A = Rb, Cs; Q = S, Se, Te)

Lykourgos Iordanidis,[†] Daniel Bilc,[‡] Subhendra D. Mahanti,[‡] and Mercouri G. Kanatzidis*[,†]

Contribution from the Department of Chemistry and Department of Physics and Astronomy, Michigan State University, East Lansing, Michigan 48824

Received January 16, 2003; E-mail: kanatzid@cem.msu.edu

Abstract: An outstanding example of structural diversity and complexity is found in the compounds with the general formula ABi_3Q_5 (A = alkali metal; Q = chalcogen). γ-$RbBi_3S_5$ (I), α-$RbBi_3Se_5$ (II), β-$RbBi_3Se_5$ (III), γ-$RbBi_3Se_5$ (IV), $CsBi_3Se_5$ (V), $RbBi_3Se_4Te$ (VI), and $RbBi_3Se_3Te_2$ (VII) were synthesized from A_2Q (A = Rb, Cs; Q = S, Se) and Bi_2Q_3 (Q = S, Se or Te) at temperatures above 650 °C using appropriate reaction protocols. γ-$RbBi_3S_5$ and α-$RbBi_3Se_5$ have three-dimensional tunnel structures while the rest of the compounds have lamellar structures. γ-$RbBi_3S_5$, γ-$RbBi_3Se_5$, and its isostructural analogues $RbBi_3Se_4Te$ and $RbBi_3Se_3Te_2$ crystallize in the orthorhombic space group *Pnma* with $a = 11.744(2)$ Å, $b = 4.0519(5)$ Å, $c = 21.081(3)$ Å, R1 = 2.9%, wR2 = 6.3% for (I), $a = 21.956(7)$ Å, $b = 4.136(2)$ Å, $c = 12.357(4)$ Å, R1 = 6.2%, wR2 = 13.5% for (IV), and $a = 22.018(3)$ Å, $b = 4.2217(6)$ Å, $c = 12.614(2)$ Å, R1 = 6.2%, wR2 = 10.3% for (VI). γ-$RbBi_3S_5$ has a three-dimensional tunnel structure that differs from the Se analogues. α-$RbBi_3Se_5$ crystallizes in the monoclinic space group *C*2/*m* with $a = 36.779(4)$ Å, $b = 4.1480(5)$ Å, $c = 25.363(3)$ Å, $\beta = 120.403(2)°$, R1 = 4.9%, wR2 = 9.9%. β-$RbBi_3Se_5$ and isostructural $CsBi_3Se_5$ adopt the space group $P2_1/m$ with $a = 13.537(2)$ Å, $b = 4.1431(6)$ Å, $c = 21.545(3)$ Å, $\beta = 91.297(3)°$, R1 = 4.9%, wR2 = 11.0% for (III) and $a = 13.603(3)$ Å, $b = 4.1502(8)$ Å, $c = 21.639(4)$ Å, $\beta = 91.435(3)°$, R1 = 6.1%, wR2 = 13.4% for (V). α-$RbBi_3Se_5$ is also three-dimensional, whereas β-$RbBi_3Se_5$ and $CsBi_3Se_5$ have stepped layers with alkali metal ions found disordered in several trigonal prismatic sites between the layers. In γ-$RbBi_3Se_5$ and $RbBi_3Se_4Te$, the layers consist of Bi_2Te_3-type fragments, which are connected in a stepwise manner. In the mixed Se/Te analogue, the Te occupies the chalcogen sites that are on the "surface" of the layers. All compounds are narrow band-gap semiconductors with optical band gaps ranging 0.4−1.0 eV. The thermal stability of all phases was studied, and it was determined that γ-$RbBi_3Se_5$ is more stable than the and α- and β-forms. Electronic band calculations at the density functional theory (DFT) level performed on α-, β-, and γ-$RbBi_3Se_5$ support the presence of indirect band gaps and were used to assess their relative thermodynamic stability.

Introduction

In the past decade, extensive investigations in the ternary and quaternary bismuth chalcogenide systems uncovered a large number of new compounds[1−14] expanding significantly this previously limited class of materials.[15] An important motivation for this work is the potential of complex bismuth chalcogenides as useful thermoelectric materials.[16] These compounds however are also of fundamental interest because of the great structural and compositional diversity they exhibit. These characteristics

[†] Department of Chemistry.
[‡] Department of Physics and Astronomy.

(1) McCarthy, T. J.; Ngeyi, S.-P.; Liao, J.-H.; DeGroot, D. C.; Hogan, T.; Kannewurf, C. R.; Kanatzidis, M. G. *Chem. Mater.* **1993**, *5*, 331−340.
(2) Chondroudis, K.; Kanatzidis, M. G. *J. Solid State Chem.* **1998**, *136*, 328−332.
(3) (a) Kanatzidis, M. G.; McCarthy, T. J.; Tanzer, T. A.; Chen, L.-H.; Iordanidis, L.; Hogan, T.; Kannewurf, C. R.; Uher, C.; Chen, B. *Chem. Mater.* **1996**, *8*, 1465−1474. (b) Chung, D.-Y.; Choi, K.-S.; Iordanidis, L.; Schindler, J. L.; Brazis, P. W.; Kannewurf, C. R.; Chen, B.; Hu, S.; Uher, C.; Kanatzidis, M. G. *Chem. Mater.* **1997**, *9*, 3060−3071.
(4) (a) Iordanidis, L.; Kanatzidis, M. G. *Angew. Chem., Int. Ed.* **2000**, *39*, 1928−1930. (b) Iordanidis, L.; Kanatzidis, M. G. *J. Am. Chem. Soc.* **2000**, *122*, 8319−8320.
(5) (a) Chung, D.-Y.; Jobic, S.; Hogan, T.; Kannewurf, C. R.; Brec, R.; Rouxel, J.; Kanatzidis, M. G. *J. Am. Chem. Soc.* **1997**, *119*, 2505−2515. (b) Chung, D.-Y.; Hogan, T.; Brazis, P.; Rocci-Lane, M.; Kannewurf, C.; Bastea, M.; Uher, C.; Kanatzidis, M. G. *Science (Washington, D.C.)* **2000**, *287*, 1024−1027.
(6) (a) Choi, K.-S.; Iordanidis, L.; Chondroudis, K.; Kanatzidis, M. G. *Inorg. Chem.* **1997**, *36*, 3804−3805. (b) Iordanidis, L.; Schindler, J. L.; Kannewurf, C. R.; Kanatzidis, M. G. *J. Solid State Chem.* **1999**, *143*, 151−162.
(7) Chung, D.-Y.; Iordanidis, L.; Rangan, K. K.; Brazis, P. W.; Kannewurf, C. R.; Kanatzidis, M. G. *Chem. Mater.* **1999**, *11*, 1352−1362.
(8) (a) Mrotzek, A.; Chung, D.-Y.; Hogan, T.; Kanatzidis, M. G. *J. Mater. Chem.* **2000**, *10*, 1667−1672. (b) Mrotzek, A.; Chung, D.-Y.; Ghelani, N.; Hogan, T.; Kanatzidis, M. G. *Chem.—Eur. J.* **2001**, *7*, 1915−1926.
(9) Iordanidis, L.; Brazis, P. W.; Kyratsi, T.; Ireland, J.; Lane, M.; Kannewurf, C. R.; Chen, W.; Dyck, J. S.; Uher, C.; Ghelani, N. A.; Hogan, T.; Kanatzidis, M. G. *Chem. Mater.* **2001**, *13*, 622−633.
(10) Hsu, K.-F.; Chung, D.-Y.; Lal, S.; Mrotzek, A.; Kyratsi, T.; Hogan, T.; Kanatzidis, M. G. *J. Am. Chem. Soc.* **2002**, *124*, 2410−2411
(11) Choe, W.; Lee, S.; O'Connell, P.; Covey, A. *Chem. Mater.* **1997**, *9*, 2025−2030.
(12) Adouby, K.; Perez Vicente, C.; Jumas, J. C.; Fourcade, R.; Abba Touré, A. *Z. Kristallogr.* **1998**, *213*, 343−349.
(13) Wang, Y. C.; DiSalvo, F. J. *Chem. Mater.* **2000**, *12*, 1011−1017.
(14) (a) Yang Y. T.; Brazis P.; Kannewurf C. R.; Ibers J. A. *J. Solid State Chem.* **2000**, *155*, 243−249. (b) Huang, F.-Q.; Somers, R. C.; McFarland, A. D.; Van Duyne R. P.; Ibers, J. A. *J. Solid State Chem.* **2003**, *174*, 334−341. (c) Ijjaali, I.; Haynes, C. L.; McFarland, A. D.; Van Duyne, R. P.; Ibers, J. A. *J. Solid State Chem.* **2003**, *174*, 257−260.

are found in the naturally occurring sulfosalts, which include many bismuth chalcogenides.[17]

There are several reasons for this unparalleled diversity and complexity. One main reason is the Bi coordination preference which is extremely malleable and can vary from 3 to 9. This is possible because of the stereochemical activity of the so-called bismuth $6s^2$ lone pair which appears to be continuously variable. Thus although bismuth atoms usually exhibit a distorted octahedral geometry they can also adopt a variety of other coordination polyhedra ranging from trigonal pyramidal, for example, in β-$CsBiS_2$,[1] to square pyramidal, for example, in $Rb_2Bi_8Se_{13}$,[9] to capped trigonal prismatic, for example, in $ALn_1\pm_xBi_4\pm_xS_8$ [6b] (A = K, Rb; Ln = La, Ce, Pr, Nd). A second reason for the structural diversity has to do with the propensity of the BiQ_6 (Q = S, Se, Te) octahedra to combine with each other by sharing edges forming a variety of building blocks or modules, the most common ones being the NaCl-, Bi_2Te_3-,[18] and CdI_2 -type[18] and occasionally the Sb_2Se_3-type fragment. Each of these modules comes in different shapes and sizes creating a plethora of structural possibilities.[19] A third reason for the structural diversity is the mixed site occupancy bismuth atoms can display with a variety of similarly sized ions such as alkali[3] or alkaline earth[13] metals, Pb,[7,10,13,17] Sn,[7b,8,13,17] or lanthanides.[6b,7b] Usually the mixed occupancy and consequently disorder are found in crystallographic sites of high (>6) coordination that connect the blocks of BiQ_6 octahedra together. Combined, the above-mentioned characteristics enable the formation of a seemingly "countless" number of phases.[19] An outstanding illustration of structural diversity and complexity is found in the six new compounds with the general formula ABi_3Q_5 (A = Rb, Cs; Q = chalcogen) reported in this work. We present the synthesis, physicochemical, spectroscopic, and structural characterization of γ-$RbBi_3S_5$, α-$RbBi_3Se_5$, β-$RbBi_3Se_5$, γ-$RbBi_3Se_5$, $CsBi_3Se_5$, and $RbBi_3Se_4Te$. These compounds crystallize in four different structure types. In this paper, we present a full discussion of these four (three new) structure types associated with the ABi_3Q_5 composition, and we contrast these with several previously known AM_3Q_5 motifs. We show that the formation of the various polymorphs is highly sensitive to the synthetic conditions.

Experimental Section

Reagents. Chemicals were used as obtained: Bi chunks (99.999% Noranda, Canada), sulfur powder, sublimed, (Spectrum Chemical Mfg. Corp., Gardena, CA), Se shots (99.999% Noranda, Canada), Rb (99.8% purity, Alfa Aesar, Ward Hill, MA), Cs (99.98% purity, Alfa Aesar, Ward Hill, MA). A_2Q (A = Rb, Cs) was prepared by a stoichiometric reaction of the corresponding alkali metal and chalcogen in liquid ammonia.

Synthesis. All manipulations of starting materials were carried out under a dry nitrogen atmosphere in a Vacuum Atmospheres Dri-Lab glovebox. The products however are air and water stable. For all compounds, the yield was practically 100% (except where stated).

Bi_2S_3. A mixture of 11.633 g (0.056 mol) of Bi and 2.677 g (0.083 mol) of S was transferred into a quartz tube, which was flame-sealed under vacuum. The tube was heated to 650 °C in 48 h, stayed at 650 °C for 2 days, and then cooled to 50 °C in 10 h. The product was ground into powder and used for further reactions.

Bi_2Se_3. A mixture of 9.407 g (0.045 mol) of Bi and 5.331 g (0.068 mol) of Se was transferred into a silica tube, which was flame-sealed under vacuum. The tube was heated to 600 °C in 12 h, stayed at 600 °C for 2 days, and then cooled to 50 °C in 6 h. The product was ground into powder and used for further reactions.

γ-$RbBi_3S_5$ (I). A mixture of 0.050 g (0.246 mmol) of Rb_2S and 0.380 g (0.739 mmol) of Bi_2S_3 was transferred to a carbon-coated silica tube which was flame-sealed under vacuum. The tube was heated for 1 day at 800 °C, then cooled to 500 °C in 30 h, and furthermore cooled to 50 °C in 10 h. The product consisted of silvery-gray thin needlelike crystals. Semiquantitative energy dispersive analysis (EDS) using a scanning electron microscope (SEM) on several needles gave an average composition of $Rb_{1.04}Bi_{2.93}S_5$.

α-$RbBi_3Se_5$ (II). A mixture of 0.060 g (0.240 mmol) of Rb_2Se and 0.456 g (0.696 mmol) of Bi_2Se_3 was transferred to a carbon crucible which was inserted into a silica tube. The tube was sealed under vacuum, heated at 780 °C for 72 h, cooled to 475 °C in 60 h, and then further cooled to 50 °C in 8 h. The product consisted of a silvery-black chunk made of hairlike thin needles. SEM/EDS analysis on several needles gave an average composition of $Rb_{1.16}Bi_{3.19}Se_5$.

β-$RbBi_3Se_5$ (III). A mixture of 0.060 g (0.240 mmol) of Rb_2Se and 0.393 g (0.600 mmol) of Bi_2Se_3 was transferred to a silica tube which was flame-sealed under vacuum. The tube was placed under the flame of a gas-oxygen torch until the sample melted, and then the tube was removed from the flame and was let to solidify. The product consisted of a silvery ingot. The above synthesis produces a mixture with γ-$RbBi_3Se_5$ (approximately 1:1 ratio) as evidenced from X-ray powder diffraction.

γ-$RbBi_3Se_5$ (IV). A mixture of 0.122 g (0.488 mmol) of Rb_2Se and 0.700 g (1.069 mmol) of Bi_2Se_3 was transferred to a silica tube which was flame-sealed under vacuum. The tube was placed under the flame of a gas-oxygen torch until the sample melted, and then the tube was removed from the flame and was let to solidify (i.e., quench). The procedure was repeated 2 more times to ensure homogeneity. The product consisted of a silvery ingot with needle morphology across its surface. SEM/EDS analysis on several needles gave an average composition of $Rb_{1.21}Bi_{3.05}Se_5$.

$CsBi_3Se_5$ (V). A mixture of 0.040 g (0.116 mmol) of Cs_2Se and 0.227 g (0.347 mmol) of Bi_2Se_3 was prepared and heated in the same manner as in compound II. The product consisted of a silvery chunk. SEM/EDS analysis on several needles gave an average composition of $Cs_{0.86}Bi_{3.04}Se_5$.

$RbBi_3Se_4Te$ (VI). A mixture of 0.050 g (0.200 mmol) of Rb_2Se, 0.305 g (0.466 mmol) of Bi_2Se_3, and 0.107 g (0.134 mmol) of Bi_2Te_3 was transferred to a carbon-coated silica tube which was flame-sealed under vacuum. The tube was heated for 3 days at 700 °C, cooled to 400 °C in 45 h, and then cooled to 50 °C in 11 h. The product consisted of silvery-gray thin needlelike crystals. SEM/EDS analysis on several needles gave an average of $Rb_{1.20}Bi_3Se_{4.05}Te_{1.02}$.

$RbBi_3Se_3Te_2$ (VII). A mixture of 0.040 g (0.160 mmol) of Rb_2Se, 0.175 g (0.267 mmol) of Bi_2Se_3, and 0.171 g (0.212 mmol) of Bi_2Te_3 was transferred to a carbon-coated silica tube which was flame-sealed under vacuum. The tube was heated for 3 days at 740 °C, cooled to

(15) (a) Glemser, O.; Filcek, M. *Z. Anorg. Allg. Chem.* **1955**, *279*, 321−323. (b) Gattow, G.; Zemann, J. *Z. Anorg. Allg. Chem.* **1955**, *279*, 324−327. (c) Golovei, M. I.; Berul, S. I.; Luzhnaya, N. P.; Peresh, E. Y. *Inorg. Mater.* **1970**, *6*, 961−964. (d) Voroshilov, Y. V.; Peresh, E. Y.; Golovei, M. I. *Inorg. Mater.* **1972**, *8*, 677−678. (e) Kanisheva, A. S.; Mikhailov, Y. N.; Lazarev, B. V.; Trippel, A. F. *Dokl. Akad. Nauk SSSR* **1980**, *252*, 96−99. (f) Schmitz, D.; Bronger, W. *Z. Naturforsch., B: Anorg. Chem., Org. Chem.* **1974**, *29*, 438−439. (g) Cordier, G.; Schäfer, H.; Schwidetzky, C. *Rev. Chim. Miner.* **1985**, *22*, 676−683. (h) Aurivillius, B. *Acta Chem. Scand., Ser. A* **1983**, *A37*, 399−407. (i) Cordier, G.; Schäfer, H.; Schwidetzky, C. *Rev. Chim. Miner.* **1985**, *22*, 631−638.
(16) Kanatzidis, M. G. *Semicond. Semimet.* **2001**, *69*, 51−100.
(17) (a) Makovicky, E. *Fortschr. Mineral.* **1981**, *59*, 137−190. (b) Makovicky, E. *Fortschr. Mineral.* **1985**, *63*, 45−89. (c) Makovicky, E. *Z. Kristallogr.* **1985**, *173*, 1−23. (d) Makovicky, E. *Neues Jahrb. Mineral., Abh.* **1989**, *160*, 269−297.
(18) Bi_2Te_3- and CdI_2-type fragments derive of course from NaCl; however, we have used this notation to differentiate between the various "cuts" of the NaCl lattice.
(19) Mrotzek A.; Kanatzidis, M. G. *Acc. Chem. Res.* **2003**, *36*, 111−119.

Table 1. Crystallographic Data for γ-$RbBi_3S_5$ (I), $CsBi_3Se_5$ (V), and $RbBi_3Se_4Te$ (VI)

empirical formula	γ-$RbBi_3S_5$ (I)	$CsBi_3Se_5$ (V)	$RbBi_3Se_4Te$ (VI)
formula weight	872.71	1154.65	1155.85
F(000)	1464	1896	1896
temperature, K	173.1(1)	299(2)	173.1(1)
crystal system	orthorhombic	monoclinic	orthorhombic
space group	*Pnma*	$P2_1/m$	*Pnma*
unit cell dimensions, Å	$a = 11.744(2)$	$a = 13.603(3)$	$a = 22.018(3)$
	$b = 4.0519(5)$	$b = 4.1502(8)$	$b = 4.2217(6)$
	$c = 21.081(3)$	$c = 21.639(4)$	$c = 12.614(2)$
		$\beta = 92.435(3)°$	
Z, volume, Å^3	4, 1003.1(2)	4, 1221.2(4)	4, 1172.5(3)
density (calculated), g/cm^3	5.78	6.28	6.55
absorption coefficient, mm^{-1}	58.28	60.90	63.83
crystal size, mm^3	$0.50 \times 0.02 \times 0.01$	$0.41 \times 0.03 \times 0.01$	$0.64 \times 0.01 \times 0.01$
θ range for data collection	1.93° to 28.79°	1.50° to 28.55°	1.85° to 26.99°
index ranges	$-15 \le h \le 11$	$-18 \le h \le 17$	$-26 \le h \le 28$
	$-5 \le k \le 5$	$-5 \le k \le 5$	$-5 \le k \le 5$
	$-28 \le l \le 27$	$-28 \le l \le 27$	$-16 \le l \le 12$
reflections collected	5867	11430	6225
independent reflections	1383 [$R_{(int)} = 0.0376$]	3254 [$R_{(int)} = 0.0713$]	1453 [$R_{(int)} = 0.1088$]
refinement method		full-matrix least-squares on F^2	
data/restraints/parameters	1383/0/56	3254/1/138	1453/0/58
goodness-of-fit on F^2	1.095	1.158	1.056
final R indices [$I > 2\sigma(I)$]	R1 = 0.0289, wR2 = 0.0633	R1 = 0.0607, wR2 = 0.1337	R1 = 0.0623, wR2 = 0.1030
R indices (all data)	R1 = 0.0428, wR2 = 0.0655	R1 = 0.0820, wR2 = 0.1428	R1 = 0.1276, wR2 = 0.1191

440 °C in 45 h, and then cooled to 50 °C in 11 h. The product consisted of silvery-gray thin needlelike crystals. SEM/EDS analysis on several needles gave an average of $Rb_{0.99}Bi_3Se_{3.17}Te_{1.97}$.

Band Structure Calculations. The electronic structure calculations were performed within density functional theory (DFT) using the full potential linearized augmented plane wave (LAPW) method implemented in WIEN 97 code.[20] Both a scalar relativistic correction and spin−orbit interaction were included. For the exchange and correlation parts of the potential, the Perdew−Burke−Ernzerhof model[21] was used, which incorporates a generalized gradient approximation (GGA). The atomic radii values (in atomic units 1 au = 0.529 Å) used in the calculations are as follows: self-consistent iterations were performed with 7, 21, and 24 k points in the reduced Brillouin zones of α-, β-, and γ-$RbBi_3Se_5$ with a cutoff between valence and core states of −6.0 Ry; convergence was assumed when the total energy difference between cycles was within 0.0001 Ry.

Electron Microscopy. Quantitative microprobe analyses of the compounds were performed with a JEOL JSM-6400V Scanning Electron Microscope (SEM) equipped with a Noran Vantage Energy Dispersive Spectroscopy (EDS) detector. Data were collected for 45 s using an accelerating voltage of 25 kV. All reported results are an average of measurements of at least three different crystals.

Differential Thermal Analysis. Differential thermal analysis (DTA) was performed with a computer-controlled thermal analyzer (Shimadzu DTA-50). Ground crystals (20−50 mg) were sealed in silica ampules under vacuum. A silica ampule containing alumina of equal mass was sealed and placed on the reference side of the detector. The samples were heated to the desired temperature at 10 °C/min, isothermed for 5 min and then cooled at 10 °C/min. The procedure was repeated to check for reproducibility. The reported DTA temperature is the peak temperature. After DTA, the samples were examined with powder X-ray diffraction.

Solid-State UV/vis Spectroscopy. Optical diffuse reflectance measurements were made at room temperature with a Shimadzu UV-3101 PC double-beam, double-monochromator spectrophotometer operating in the 200−2500 nm region. The instrument was equipped with an integrating sphere. $BaSO_4$ powder was used as reference (100% reflectance). Absorption data were calculated from the reflectance data using the Kubelka−Munk function.[22]

Infrared Spectroscopy. Optical band gaps were determined from diffuse reflectance measurements that were made on the finely ground sample at room temperature. The spectrum was recorded in the infrared region (6000−400 cm^{-1}) with the use of a Nicolet MAGNA-IR 750 spectrometer equipped with a Collector Diffuse Reflectance of Spectra-Tech. Inc. The band gap was determined as described elsewhere.[3b]

Powder X-ray Diffraction. The compounds were examined by X-ray powder diffraction to check for phase purity and for identification. Powder patterns were obtained using a Rigaku−Denki/Rw400F2 (Rotaflex) rotating-anode powder diffractometer and a CPS 120 INEL X-ray powder diffractometer equipped with a position-sensitive detector. The purity and homogeneity of all phases were confirmed by comparison of X-ray diffraction patterns to those calculated from crystallographically determined atomic coordinates using the CERIUS^2 software.[23]

Single-Crystal X-ray Crystallography. A Bruker SMART Platform CCD diffractometer was used for data collection. Several different sets of frames covering a random area of the reciprocal space were collected using 0.3° steps in ω at a detector-to-sample distance of ∼5 cm. The SMART[24] software was used for data acquisition, and SAINT,[24] for data extraction. The absorption correction was done with SADABS,[24] and the structure solution (direct methods) and refinement was done with the SHELX97/SHELXTL[24] package of crystallographic programs. The fractional atomic coordinates and thermal atomic displacement parameters of all compound were deposited in the Supporting Information.

γ-$RbBi_3S_5$ (I). A hemisphere of data was collected (1282 frames) with an exposure time of 40 s per frame. The final cell was calculated from 2343 [$I > 8\sigma(I)$] reflections from the actual data collection (Table 1). The resolution of the data set was 0.74 Å. Three bismuth atoms, one rubidium, and five sulfur atoms were found to sit on a crystallographic mirror plane. After refinement, the R1 and wR2 values were 3.7% and 8.1%, respectively. All the atoms were refined anisotropically (R1 = 2.9%, wR2 = 6.3%).

α-$RbBi_3Se_5$ (II). Over a hemisphere of data was collected (1397 frames) with an exposure time of 35 s per frame. The final cell was

(20) Blaha, P.; Schwarz, K.; Luitz, J. *WIEN 97*: A Full Potential Linearized Augmented Plane Wave Package for Calculating Crystal Properties, Vienna University of Technology, Getreidemarkt 9/158, A-1060 Vienna, Austria.
(21) Perdew, J. P.; Burke, S.; Ernzerhof, M. *Phys. Rev. Lett.* **1996**, *77*, 3865.
(22) (a) Wendlandt, W. W.; Hecht, H. G. *Reflectance Spectroscopy*; Interscience Publishers: New York, 1966. (b) Kotüm, G. *Reflectance Spectroscopy*; Springer-Verlag: New York, 1969. (c) Tandon, S. P.; Gupta, J. P. *Phys. Status Solidi* **1970**, *38*, 363−367.
(23) *CERIUS*^{2}, version 3.8.; Molecular Simulations Inc.: Cambridge, U.K., 1999.
(24) *SMART*, v4 and 5 1996−1999, *SAINT*, v4, 5, and 6 1994−1999, *SADABS*, *SHELXTL V-5*; Bruker Analytical Xray Systems Inc.: Madison, WI 53719 USA.

Table 2. Crystallographic Data for α-$RbBi_3Se_5$ (II), β-$RbBi_3Se_5$ (III), and γ-$RbBi_3Se_5$ (IV)

	α-$RbBi_3Se_5$ (II)	β-$RbBi_3Se_5$ (III)	γ-$RbBi_3Se_5$ (IV)
empirical formula			
formula weight	1107.21	1107.21	1107.21
F(000)	5472	1824	1824
temperature, K	293(2)	298(2)	297(2)
crystal system	monoclinic	monoclinic	orthorhombic
space group	*C2/m*	$P2_1/m$	*Pnma*
unit cell dimensions, Å	$a = 36.779(4)$	$a = 13.537(2)$	$a = 21.956(7)$
	$b = 4.1480(5)$	$b = 4.1431(6)$	$b = 4.136(1)$
	$c = 25.363(3)$	$c = 21.545(3)$	$c = 12.357(4)$
	$\beta = 120.403(2)°$	$\beta = 91.297(3)°$	
Z, volume, Å^3	12, 3337.3(7)	4, 1208.0(3)	4, 1122.0(6)
density (calculated), g/cm^3	6.61	6.09	6.56
absorption coefficient, mm^{-1}	67.98	62.60	67.40
crystal size, mm^3	0.50 × 0.02 × 0.02	0.40 × 0.05 × 0.01	0.13 × 0.01 × 0.01
θ range for data collection	1.64° to 28.77°	1.50° to 27.91°	1.86° to 27.11°
index ranges	$-46 \le h \le 47$	$-17 \le h \le 17$	$-26 \le h \le 28$
	$-5 \le k \le 5$	$-5 \le k \le 7$	$-2 \le k \le 5$
	$-34 \le l \le 22$	$-28 \le l \le 28$	$-13 \le l \le 15$
reflections collected	11 280	12 148	6433
independent reflections	4492 [$R_{(int)} = 0.0575$]	3245 [$R_{(int)} = 0.0638$]	1417 [$R_{(int)} = 0.1239$]
refinement method		full-matrix least-squares on F^2	
data/restraints/parameters	4492/0/165	3245/1/140	1417/0/56
goodness-of-fit on F^2	0.954	0.985	0.993
final R indices [$I > 2\sigma(I)$]	R1 = 0.0488, wR2 = 0.0988	R1 = 0.0490, wR2 = 0.1099	R1 = 0.0617, wR2 = 0.1353
R indices (all data)	R1 = 0.0853, wR2 = 0.1070	R1 = 0.0928, wR2 = 0.1221	R1 = 0.1372, wR2 = 0.1554

calculated from 2540 [$I > 10\sigma(I)$] reflections (Table 2). The resolution of the data set was 0.74 Å. Ten bismuth atoms, three rubidium, and fifteen selenium atoms were found to sit on a crystallographic mirror plane. After refinement, the R1 and wR2 values were 5.7% and 12.3%, respectively. All the atoms were refined anisotropically (R1 = 4.9%, wR2 = 9.9%).

β-$RbBi_3Se_5$ (III). A full hemisphere of data was collected (2229 frames) with an exposure time of 50 s per frame. The final cell was calculated from 3510 [$I > 8\sigma(I)$] reflections (Table 2). The resolution of the data set was 0.76 Å. Because the compound is isostructural with compound V, (see below) the fractional atomic coordinates for the Bi and Se sites from compound V were used for initial refinement of the structure. After refinement, the R1 and wR2 values were 9.6% and 28.9%, respectively. At this stage of the refinement, six peaks appear in the electron density map sitting between the layers. These peaks were assigned as Rb, and their occupancy was refined (R1 = 7.7%, wR2 = 11.9%). All the atoms were refined anisotropically (R1 = 4.9%, wR2 = 11.0%). At this point, the crystallographically refined formula was $Rb_{1.005}Bi_3Se_5$, extremely close to the ideal formula of $RbBi_3Se_5$.

γ-$RbBi_3Se_5$ (IV). A hemisphere of data was collected (1288 frames) with an exposure time of 80 s per frame. The final cell was calculated from 959 [$I > 8\sigma(I)$] reflections (Table 2). The resolution of the data set was 0.78 Å. Three bismuth atoms, one rubidium, and five selenium atoms were found to sit on a crystallographic mirror plane. After refinement, the R1 and wR2 values were 7.5% and 20.5%, respectively. All the atoms were refined anisotropically (R1 = 6.2%, wR2 = 13.7%).

$CsBi_3Se_5$ (V). A full sphere of data was collected (2060 frames) with an exposure time of 30 s per frame. The final cell was calculated from 4679 [$I > 10\sigma(I)$] reflections (Table 1). The resolution of the data set was 0.74 Å. Initial attempts to solve the structure in $P2_1/m$ were not successful. The symmetry was lowered, and the structure was solved successfully in *Pm* (only the Bi−Se framework was located). At a subsequent stage using a missing center utility in teXsan,[25] a center of symmetry was found, the extra Bi and Se atoms were deleted, and the structure was refined in $P2_1/m$. After refinement, the R1 and wR2 values were 18.1% and 41.1%, respectively. Six peaks appear in the electron density map sitting in the space between the layers; these were assigned as Cs, and their occupancy was refined (R1 = 10.9%, wR2 = 30.7%). All the atoms were refined anisotropically (R1 = 6.1%, wR2 = 13.4%). The formula at this point was $Cs_{1.04}Bi_3Se_5$, very close to the ideal $CsBi_3Se_5$.

$RbBi_3Se_4Te$ (VI). A hemisphere of data was collected (1289 frames) with an exposure time of 45 s per frame. The final cell was calculated from 1110 [$I > 10\sigma(I)$] reflections (Table 1). The resolution of the data set was 0.75 Å. Three bismuth atoms, one rubidium, and five "selenium" atoms were found to sit on a crystallographic mirror plane. After refinement, the R1 and wR2 values were 8.6% and 16.8%, respectively. Two of the selenium atoms had very small isotropic displacement parameters, $U_{iso} \approx 0.002-0.005$ Å^2, compared to that of the other three Se atoms which varied between 0.011 and 0.014 Å^2. These two Se atoms were disordered with Te (R1 = 7.7%, wR2 = 14.4%). All the atoms were refined anisotropically (R1 = 6.2%, wR2 = 10.3%). To check if the other three Se sites contained Te, the Se occupancies were refined. For two of the sites, the occupancy increased slightly to 0.52 (0.500 for full occupancy), and, for the third, atom did not change at all (remained at 0.5). At the same time, there was no significant change in the *R* values; therefore, the remaining three chalcogen sites were left fully occupied by Se.

Results and Discussion

The following sections first describe the synthesis, thermal stability, relative stability, and optical absorption properties of the ABi_3Q_5 set of compounds followed by a limited discussion of band structure calculations aimed at understanding the nature of the band gap and observed relative stability in the $RbBi_3Se_5$ polymorphs. The new structure types are then described in detail, and their inter-relationships are discussed and placed in context with previously reported structure types of this stoichiometry.

Synthesis and Thermal Analysis. γ-$RbBi_3S_5$ was synthesized by reacting Rb_2S and Bi_2S_3 in a 1:3 molar ratio. This phase however forms from a wide range of ratios. During our investigations, the only other phase we encountered in the Rb/Bi/S system was $RbBiS_2$.[15d] The α-form of $RbBi_3S_5$ has been reported in a brief and sketchy report three decades ago,[15f] while β-$RbBi_3S_5$ can only be made via an ion-exchange reaction using KBi_3S_5 and RbCl.[2] After repeated attempts, we were unable to synthesize even traces of α-$RbBi_3S_5$ for which no synthesis has been published.

(25) *teXsan*, v1.8; Molecular Structure Corporation: The Woodlands, TX 77831 USA, 1996.

α-$RbBi_3Se_5$ was discovered initially as a byproduct in the synthesis of $Rb_3Bi_7Se_{12}$.[26] We noticed that prolonged heating periods (> 60 h at 750 °C) of $Rb_3Bi_7Se_{12}$ resulted in well-shaped crystal rods of α-$RbBi_3Se_5$ on its surface. Later a rational synthesis was developed by combining Rb_2Se and Bi_2Se_3 in a 1:2.9 molar ratio at 780 °C. $CsBi_3Se_5$ was synthesized from a 1:3 molar ratio of Cs_2Se/Bi_2Se_3 at 780 °C.

$RbBi_3Se_4Te$ was initially discovered in an attempt to replace some of the Se atoms in $Rb_2Bi_8Se_{13}$ [9] with Te. The replacement did not occur, and instead, a new phase was formed with mixed Se/Te occupancy. A rational synthesis was devised to obtain $RbBi_3Se_4Te$ by reacting Rb_2Se with Bi_2Se_3 and Bi_2Te_3 in a 3:7:2 molar ratio.

Since the above compounds have the same formula, we looked for a system where all three different structures existed in the same composition. This was only possible for the Rb/Bi/Se system. In the Cs/Bi/Se system, only $CsBi_3Se_5$ (isostructural with β-$RbBi_3Se_5$) could be obtained. In the A/Bi/Te systems (A = Rb, Cs), no compound with the formula ABi_3Te_5 (A = Rb, Cs) was found; instead, $Rb_{0.5}Bi_{1.83}Te_3$ [27] and $CsBi_4Te_6$ [5b] are the most stable products.

The "all Se" analogue of $RbBi_3Se_4Te$, γ-$RbBi_3Se_5$ was prepared with the quenching technique described in the synthesis section. β-$RbBi_3Se_5$ was synthesized also with the quenching technique but only as a mixture with γ-$RbBi_3Se_5$ (~1:1 ratio) as evidenced from X-ray powder diffraction. Although we tried a number of ways to synthesize β-$RbBi_3Se_5$ in pure form, we were not successful probably due to its metastable character.

We also investigated the amount of additional Te that the $RbBi_3Se_4Te$ structure could accommodate. We found that the structure remains stable up to two Te atoms per formula (i.e., $RbBi_3Se_3Te_2$) as evidenced by powder X-ray diffraction (shifting of the diffraction peaks to slightly higher *d* spacings as expected) and EDS/SEM analysis ($Rb_{0.99}Bi_3Se_{3.17}Te_{1.97}$). When the amount of Te increases to >2 Te atoms per formula, the diffraction pattern changes indicating a different phase, which is under investigation.

The differential thermal analysis (DTA) studies indicate that γ-$RbBi_3S_5$ melts congruently at 697 °C, whereas γ-$RbBi_3Se_5$ melts at 675 °C but transforms on cooling to $Rb_2Bi_8Se_{13}$ and Rb_2Se indicating its metastable character. It is interesting to note that unlike γ-$RbBi_3Se_5$ the isostructural $RbBi_3Se_4Te$ is a congruently crystallizing compound at 642 °C. This may be due to the lack of competing ≪$Rb_2Bi_8Te_{13}$≫ phase. α-$RbBi_3Se_5$ melts at ~680 °C and converts to a mixture of γ-$RbBi_3Se_5$ and $Rb_2Bi_8Se_{13}$. We also examined the thermal behavior of a mixture of β- and γ-$RbBi_3Se_5$ and found that at 678 °C it converts to a mixture of γ-$RbBi_3Se_5$ and $Rb_2Bi_8Se_{13}$. $CsBi_3Se_5$ melts at 686 °C converting to $CsBi_{3.67}Se_6$.[9]

Annealing studies were also performed to check if any of the three phases α-, β-, γ-$RbBi_3Se_5$ interconvert in the solid state. The samples of α-, β+γ-mixture, β-, and $CsBi_3Se_5$ were annealed for 60 h at 480 °C. The results were identical to those of the differential thermal analysis. That is, α-$RbBi_3Se_5$ converts to γ-$RbBi_3Se_5$ and $Rb_2Bi_8Se_{13}$, the β- and γ-$RbBi_3Se_5$ mixture converts to a mixture of γ-$RbBi_3Se_5$ and $Rb_2Bi_8Se_{13}$, γ-$RbBi_3Se_5$ transforms to $Rb_2Bi_8Se_{13}$, and $CsBi_3Se_5$ converts to $CsBi_{3.67}Se_6$.We conclude that γ-$RbBi_3Se_5$ is the most stable among the three forms, although it too finally decomposes to $Rb_2Bi_8Se_{13}$.

(26) Iordanidis, L.; Kanatzidis, M. G. Manuscript in preparation.
(27) Chung, D.-Y.; Kanatzidis, M. G. Work in progress.

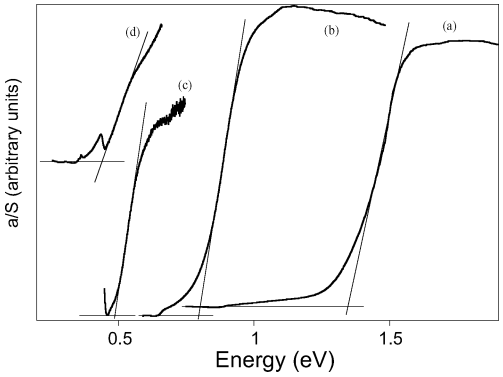

Figure 1. Solid-state UV/vis and infrared absorption spectra showing band-gap transitions for (a) γ-$RbBi_3S_5$ (b) γ-$RbBi_3Se_5$, (c) β-$RbBi_3Se_5$, and (d) α-$RbBi_3Se_5$. The band gaps in each case are estimated from the crossing point of the solid lines shown in each spectrum.

Spectroscopy. Optical and infrared spectroscopy detected sizable energy gaps indicating that all materials are semiconductors. As expected, the sulfide compound γ-$RbBi_3S_5$ exhibits the widest energy band gap at ~1.34 eV; see Figure 1. γ-$RbBi_3Se_5$ has a band gap of 0.8 eV, while its isostructural $RbBi_3Se_4Te$ analogue has a lower band gap of 0.5 eV. This is in agreement with the fact that the incorporation of the heavier Te atoms into a selenide compound is expected to lower the band gap. $CsBi_3Se_5$ has a band gap of 0.46 eV and the isostructural β-$RbBi_3Se_5$ has a similar band gap of 0.48 eV, while α-$RbBi_3Se_5$ has a gap of 0.43 eV.

The largest gap of γ-$RbBi_3Se_5$ is due to its low dimensionality and small thickness of its $[Bi_3Se_5]^-$ layers. β-$RbBi_3Se_5$ which also has a two-dimensional structure has thicker layers which favor band broadening and consequently a smaller gap. α-$RbBi_3Se_5$ has a three-dimensional structure and its band gap is very similar to that of the β-$RbBi_3Se_5$. The previously reported KBi_3S_5 and β-$RbBi_3S_5$ have a band gap of ~1.2 eV, a value comparable to that of γ-$RbBi_3S_5$.

Band Structure Calculations. For a qualitative discussion of the influence of the crystal structure on the electronic structure, properties and the relative stability of α-, β-, and γ-$RbBi_3Se_5$, we performed electronic band structure calculations in the density functional theory (DFT) formalism.[20] It is well-known that DFT calculations cannot quantitatively determine the band-gap energies, but they are reasonably good in capturing relative trends in a series of isomeric and isoelectronic species.

The band structures of α-, β-, and γ-$RbBi_3Se_5$ are shown in Figure 2. As expected for valence-precise semiconductors, well-defined energy band gaps exist and are summarized in Table 3. The band gaps of α-, β-, and γ-$RbBi_3Se_5$ are all indirect with sizes of 0.39, 0.22, and 0.56 eV, respectively. The trend agrees well with the experimental data (see Table 3), though the measured values are slightly different than those calculated. According to the calculated total energies of the $RbBi_3Se_5$ polymorphs, the γ-form with the least complex structure is predicted to be the most stable, and this corresponds well to our experimental observations.

Total density of states (DOS) plots for all α, β, γ-$RbBi_3Se_5$ (not shown) are similar and show that the energy levels near the Fermi level are dominantly of Bi 4s and 4p and Se 4p character. Mixing of these orbitals gives rise to strong Bi−Se

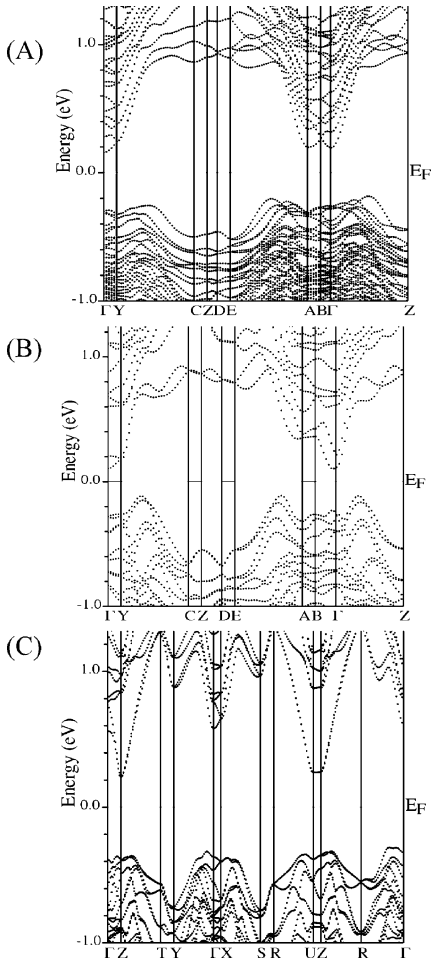

Figure 2. Band structure plots of (a) α-$RbBi_3Se_5$ (E_g = 0.39 eV), (b) β-$RbBi_3Se_5$ (E_g = 0.22 eV), and (c) γ-$RbBi_3Se_5$ (E_g = 0.56 eV). Monoclinic symmetry (α, β) points: Γ = (0,0,0); Y = (0,0.5,0); C = (0,0.5,0.5); Z = (0,0,0.5); D = (0.5,0,0.5); E = (0.5,−0.5,0.5); A = (0.5,−0.5,0); B = (0.5,0,0). Orthorhombic symmetry (Y) points: Γ = (0,0,0); Z = (0,0,0.5); T = (0,0.5,0.5); Y = (0,0.5,0); X = (0.5,0,0); S = (0.5,0.5,0); R = (0.5,0.5,0.5); U = (0.5,0,0.5).

Table 3. Experimental and Calculated Band Gaps and Total Energies of the Polymorphs of $RbBi_3Se_5$

	α-$RbBi_3Se_5$	β-$RbBi_3Se_5$	γ-$RbBi_3Se_5$
E_g (experimental) [eV]	0.43	0.48	0.80
E_g (calculated) [eV]	0.39	0.22	0.56
total energy per formula[a] at Fermi level [eV][b]	0.0	+3.294	−0.449

[a] Normalized for the same number of atoms. [b] The total energies are relative to that of α-$RbBi_3Se_5$. The calculated absolute energy of this compound is −2 173 579.835 eV.

interactions. Bi s and Se p orbitals contribute to the highest occupied state and Bi p and Se p orbitals to the lowest unoccupied state, although the Bi p contribution is dominant in the latter. In general, the states above the Fermi level have mainly Bi p, some Se p, and very little Bi s orbital character. Based on these calculations, the optical absorption associated with the band-gap transition in these compounds can be understood in terms of a charge transfer excitation from Se p-type orbitals in the valence band to a predominantly p orbital of Bi in the conduction band.

Structure Description. A. γ-$RbBi_3S_5$ (I). This compound is isostructural with $CsBi_3S_5$ [15e] but different from α-$RbBi_3S_5$ [15f] and β-$RbBi_3S_5$. The structure is a dense covalent $[Bi_3S_5]^-$ three-dimensional framework that creates adequate space in the form of parallel tunnels for the charge balancing Rb^+ ions; see Figure 3. The $[Bi_3S_5]^-$ framework consists of Bi_2Te_3-type infinite rods three Bi octahedra wide that are connected with each other by sharing corners. Each rod is connected with four other rods, and the Bi_2Te_3-type rods are arranged in a zigzag fashion. The zigzag arrangement is found also in other bismuth chalcogenides, such as $CsBi_{3.67}Se_6$,[9] where a different building block is arranged in a similar fashion.

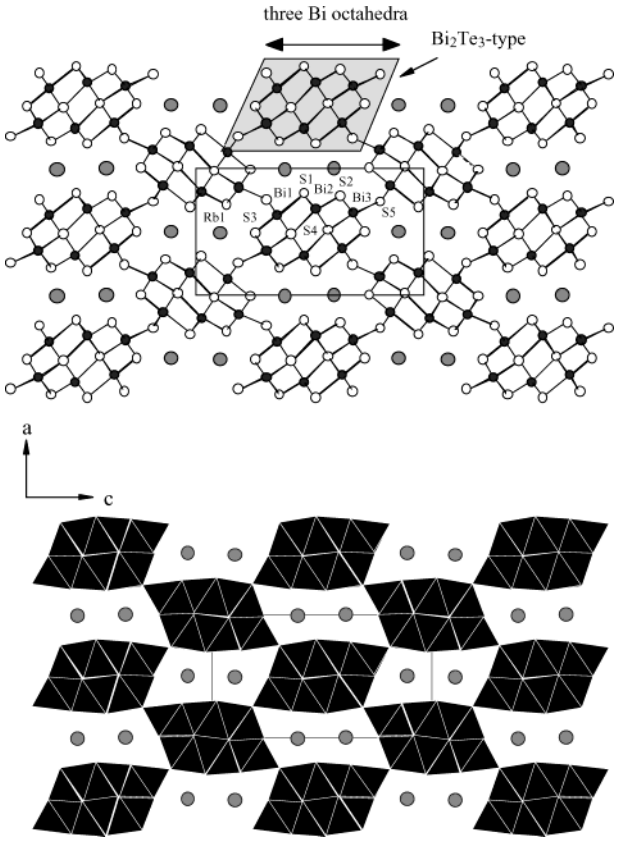

Figure 3. Projection of the structure of γ-$RbBi_3S_5$ down the *b*-axis (top). The shaded area indicates the three bismuth octahedra wide Bi_2Te_3-type building block. The block has the shape of an infinite rod, and it is viewed here down the infinite axis. Polyhedral representation of the structure of γ-$RbBi_3S_5$ down the *b*-axis (bottom).

The Bi atoms in the Bi_2Te_3-type block have a distorted octahedral coordination; see Table 4. Bi(1) and Bi(2) are distorted toward a trigonal pyramid having three short bonds trans to three longer bonds; for example, Bi(1) has one bond at 2.626(3) Å, two bonds at 2.669(2) Å, two bonds at 2.986(2) Å, and one bond at 3.227(4) Å. Bi(3) is less distorted with distances varying between 2.781(3) and 2.872(3) Å and angles between 84.33(8)° and 99.38(8)°. The Rb has a bicapped trigonal prismatic coordination with distances varying between 3.275(4) and 3.792(3) Å.

The structure of γ-$RbBi_3S_5$ is dramatically different from the structure of α-$RbBi_3S_5$;[15f,28] compare Figures 3 and 4. The

(28) The S^{2-} ion in the middle of the channels has two more sulfur atoms around it in a linear fashion at 2.789 Å away. These distances are too long to be S−S bonds. Furthermore the same S^{2-} ion is only 2.467 Å away from the Rb cations, a distance too short for Rb−S bonds. All these features together with the fact that the reported *R* value is 10% imply that most probably the structure is not correct and does not exist. No temperature factors were given in the paper; see ref 15f.

Table 4. Bond Distances (Å) and Selected Angles (deg) for γ-$RbBi_3S_5$

Bi(1)−S(3)	2.626(3)	S(5)−Bi(1)−S(1)	85.96(9)
Bi(1)−S(5)	2.669(2) × 2	S(5)−Bi(1)−S(5)	98.8(1)
Bi(1)−S(4)	2.986(2) × 2	S(3)−Bi(1)−S(1)	180.0(1)
Bi(1)−S(1)	3.227(4)		
Bi(2)−S(2)	2.572(3)	S(4)−Bi(2)−S(4)	79.34(8)
Bi(2)−S(1)	2.719(2) × 2	S(1)−Bi(2)−S(4)	96.70(9)
Bi(2)−S(4)	3.015(3) × 2	S(2)−Bi(2)−S(4)	163.0(1)
Bi(2)−S(4)	3.232(3)		
Bi(3)−S(4)	2.781(3)	S(5)−Bi(3)−S(3)	84.33(8)
Bi(3)−S(5)	2.786(3)	S(5)−Bi(3)−S(2)	99.38(9)
Bi(3)−S(3)	2.794(2) × 2	S(4)−Bi(3)−S(5)	170.7(1)
Bi(3)−S(2)	2.872(3) × 2		
Rb(1)−S(5)	3.275(4)		
Rb(1)−S(2)	3.316(3) × 2		
Rb(1)−S(1)	3.498(3) × 2		
Rb(1)−S(1)	3.635(4)		
Rb(1)−S(3)	3.792(3) × 2		

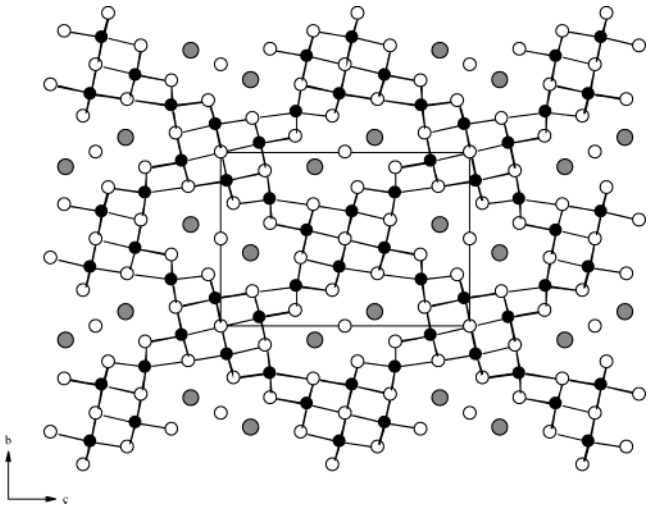

Figure 4. Projection of the structure of α-$RbBi_3S_5$ down the *a*-axis. Adapted using atomic coordinates reported in ref 15f.

α-structure has the unusual feature of having an S^{2-} ion sitting in tunnels between the Rb atoms. In a way, this structure can be described as a neutral tunnel framework of "Bi_2S_3" stuffed with Rb_2S. Unfortunately, we could not reproduce the synthesis of this seemingly novel phase.[28] A comparison with the β-$RbBi_3S_5$ structure will be discussed later.

B. α-$RbBi_3Se_5$ (II). This compound adopts a new three-dimensional structure which consists of parallel Bi_2Te_3-type and CdI_2-type infinite rod type fragments; see Figure 5. The CdI_2-type fragments adopt two orientations, parallel and perpendicular to the *a*-axis, essentially forming the walls of tunnels that have square or rectangular cross-sections. At the corners of the tunnels, one set of Bi_2Te_3-type fragments forms where those tunnels join, whereas another set of such fragments "stuffs" them. Furthermore, each tunnel contains six Rb atoms. Figure 5b shows a polyhedral representation of the structure of α-$RbBi_3Se_5$ where most of the Bi_2Te_3-type rods filling the rectangular tunnels have been removed in order to reveal and highlight the rectangular tunnels.

All Bi atoms have octahedral coordination with varying degrees of distortion (Table 5). The least distorted are Bi(4) located at the cell corners in the CdI_2-type fragment with Bi−Se varying between 2.934(3) and 2.945(2) Å and Se−Bi−Se angles varying between 88.95(6)° and 91.05(6)° and

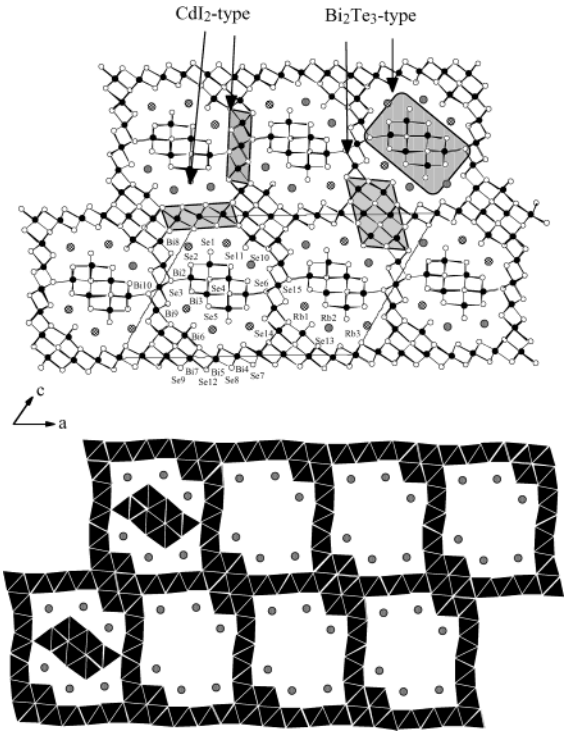

Figure 5. Projection of the structure of α-$RbBi_3Se_5$ down the *b*-axis (top). The shaded areas indicate the Bi_2Te_3- and CdI_2-type building blocks. Polyhedral representation of the structure of α-$RbBi_3Se_5$ (bottom). Most of the Bi_2Te_3-type fragments has been removed to show the large rectangular tunnels.

Bi(10) located in other CdI_2-type fragments at the center of the cell with Bi−Se distances varying between 2.904(3) and 2.939(2) Å and Se−Bi−Se angles varying between 88.74(6)° and 91.26(6)°. Bi(7) is slightly more distorted with two bonds at 2.878(2) Å, two between 2.971(3) and 2.985(3) Å, and two at 3.015(2) Å. One kind of common octahedral distortion is toward a trigonal pyramid where the metal center moves toward one octahedron face. In this distortion, there are three short bonds trans to three longer ones. Sometimes the three short bonds are almost equal, and as a result, the three trans lying longer bonds will also be equal in distance. At other times, one of the three short bonds is shorter than the other two, and as a result, the corresponding long bond is longer than the other two. The environment of the Bi(1), Bi(3), Bi(5), Bi(8), and Bi(9) octahedra belong to this category. For example, Bi(1) has three short bonds between 2.807(2) and 2.812(3) Å trans to three longer bonds between 3.149(3) and 3.166(2) Å, while Bi(3) has one short bond at 2.738(3) Å, two short bonds at 2.822(2) Å, two longer bonds at 3.145(2) Å, and an even longer one at 3.211(3) Å. The distortion of Bi(2) can be described as square pyramid with four almost equal basal bonds between 2.916(2) and 2.975(2) Å and one short bond at 2.794(3) Å forming the apex trans to a longer one at 3.104(3). Bi(6) has three sets of equal distances, one set of two at 2.812(2) Å, another at 2.926(3) Å and another at 3.114(2) Å.

The three Rb atoms are eight coordinate with a bicapped trigonal prismatic coordination. The Rb−Se distances vary between 3.409(3)−3.590(3) Å for Rb(1), 3.477(3)−3.712(3) Å for Rb(2) and 3.487(4)−3.973(4) Å for Rb(3).

C. β-$RbBi_3Se_5$ (III) and $CsBi_3Se_5$ (V). Because these two compounds are isostructural, only $CsBi_3Se_5$ will be described

Table 5. Bond Distances (Å) and Selected Angles (deg) for α-$RbBi_3Se_5$

Bi(1)−Se(1)	2.807(2) × 2	Se(4)−Bi(1)−Se(4)	81.86(7)
Bi(1)−Se(2)	2.812(3)	Se(1)−Bi(1)−Se(1)	95.27(9)
Bi(1)−Se(5)	3.149(3)	Se(2)−Bi(1)−Se(5)	170.69(8)
Bi(1)−Se(4)	3.166(2) × 2		
Bi(2)−Se(4)	2.794(3)	Se(3)−Bi(2)−Se(6)	82.50(7)
Bi(2)−Se(2)	2.916(2) × 2	Se(2)−Bi(2)−Se(6)	96.42(7)
Bi(2)−Se(3)	2.975(2) × 2	Se(4)−Bi(2)−Se(6)	168.20(8)
Bi(2)−Se(6)	3.104(3)		
Bi(3)−Se(3)	2.738(3)	Se(4)−Bi(3)−Se(4)	84.94(6)
Bi(3)−Se(5)	2.822(2) × 2	Se(3)−Bi(3)−Se(5)	96.18(7)
Bi(3)−Se(4)	3.145(2) × 2	Se(3)−Bi(3)−Se(4)	168.83(8)
Bi(3)−Se(4)	3.211(3)		
Bi(4)−Se(7)	2.934(3) × 2	Se(7)−Bi(4)−Se(8)	88.95(6)
Bi(4)−Se(8)	2.945(2) × 4	Se(7)−Bi(4)−Se(8)	91.05(6)
		Se(8)−Bi(4)−Se(8)	180.0
Bi(5)−Se(8)	2.798(3)	Se(7)−Bi(5)−Se(9)	84.77(6)
Bi(5)−Se(7)	2.862(2) × 2	Se(8)−Bi(5)−Se(12)	97.15(7)
Bi(5)−Se(12)	3.084(2) × 2	Se(7)−Bi(5)−Se(12)	168.76(8)
Bi(5)−Se(9)	3.095(3)		
Bi(6)−Se(11)	2.812(2) × 2	Se(13)−Bi(6)−Se(13)	83.53(7)
Bi(6)−Se(10)	2.926(3)	Se(11)−Bi(6)−Se(11)	95.07(8)
Bi(6)−Se(9)	2.930(3)	Se(10)−Bi(6)−Se(9)	169.22(8)
Bi(6)−Se(13)	3.114(2) × 2		
Bi(7)−Se(9)	2.878(2) × 2	Se(13)−Bi(7)−Se(13)	84.77(6)
Bi(7)−Se(12)	2.971(3)	Se(12)−Bi(7)−Se(13)	94.66(6)
Bi(7)−Se(13)	2.985(3)	Se(9)−Bi(7)−Se(13)	173.95(7)
Bi(7)−Se(13)	3.015(2) × 2		
Bi(8)−Se(14)	2.691(3)	Se(10)−Bi(8)−Se(13)	83.54(6)
Bi(8)−Se(10)	2.872(2) × 2	Se(14)−Bi(8)−Se(12)	95.34(7)
Bi(8)−Se(12)	3.086(2) × 2	Se(10)−Bi(8)−Se(12)	170.01(8)
Bi(8)−Se(13)	3.278(3)		
Bi(9)−Se(6)	2.838(3)	Se(10)−Bi(9)−Se(14)	83.52(6)
Bi(9)−Se(15)	2.866(2) × 2	Se(6)−Bi(9)−Se(14)	104.51(7)
Bi(9)−Se(10)	3.044(3)	Se(15)−Bi(9)−Se(14)	163.88(8)
Bi(9)−Se(14)	3.061(2) × 2		
Bi(10)−Se(15)	2.904(3) × 2	Se(15)−Bi(10)−Se(6)	88.74(6)
Bi(10)−Se(6)	2.939(2) × 4	Se(15)−Bi(10)−Se(6)	91.26(6)
		Se(15)−Bi(10)−Se(15)	179.998(1)
Rb(1)−Se(3)	3.409(3) × 2		
Rb(1)−Se(5)	3.475(4)		
Rb(1)−Se(15)	3.485(3) × 2		
Rb(1)−Se(10)	3.529(4)		
Rb(1)−Se(11)	3.590(3) × 2		
Rb(2)−Se(1)	3.477(3) × 2		
Rb(2)−Se(9)	3.489(4)		
Rb(2)−Se(11)	3.638(3) × 2		
Rb(2)−Se(5)	3.663(4)		
Rb(2)−Se(7)	3.712(3) × 2		
Rb(3)−Se(1)	3.487(4)		
Rb(3)−Se(14)	3.497(3) × 2		
Rb(3)−Se(8)	3.583(3) × 2		
Rb(3)−Se(2)	3.612(3) × 2		
Rb(3)−Se(12)	3.973(4)		

in detail. These have layered structures with slabs assembled from NaCl-type fragments; see Figure 6. This fragment repeats creating stepped layers. The space between the layers is constricted creating two different tunnels, one small that can accommodate snuggly the Cs(1) atom and a larger one where the remaining Cs atoms are found disordered over several different trigonal prismatic sites.

The location and behavior of the alkali atoms deserve special mention. All the Cs atoms residing in the tunnels between the layers are partially occupied. Cs(1) is located in the smaller tunnels between the layers having a tricapped trigonal prismatic coordination with Cs−Se distances varying between 3.311(6) and 4.072(5) Å. It generates a symmetry equivalent 2.0856(8) Å away and so is only 50% occupied. Cs(2) and Cs(4) have bicapped and monocapped trigonal prismatic coordination, respectively, sitting in the edges of the large cavity area between the layers while Cs(3), Cs(5), and Cs(6) are six coordinate having a trigonal prismatic coordination. The equivalent isotropic displacement parameters of the Cs atoms with the exception of Cs(1) are large. The smaller temperature factor of Cs(1) can be rationalized if we consider that the Cs(1) crystallographic site fits precisely the size of Cs^+ and also acts as a pillar between the Bi−Se layers. In contrast, the Cs(2)−Cs(6) atoms sit in a tunnel that is slightly too large and are free to move about, giving rise to a rattling motion and large displacement parameters. A similar situation is also observed in KBi_3S_5 [2] where the K atoms reside in oversized tunnels. This makes the ions mobile and gives rise to good ion-exchange properties. Based on these facts, we anticipate that the Cs(2)−Cs(6) atoms could be ion exchangeable.

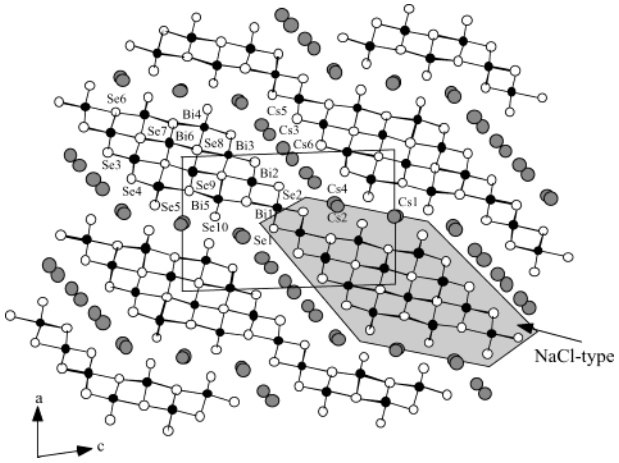

Figure 6. Projection of the structure of $CsBi_3Se_5$ (also adopted by β-$RbBi_3Se_5$) down the *b*-axis. The shaded area indicates the NaCl-type building blocks.

The Bi atoms in the framework have distorted octahedral coordination (Table 6). The Bi(6) atom at the center of the NaCl-type is the least distorted with Bi−Se bond distances varying between 2.884(2) and 3.024(2) Å and Se−Bi−Se angles varying between 86.67(7)° and 92.67(6)°. This feature has been observed in other bismuth selenides where the atoms in the center of the NaCl-type fragment exhibit the smallest distortion.[9] Bi(1) has a distortion toward a square pyramid with four nearly in-plane bonds at 2.941(2)−2.980(2) Å, one Bi−Se bond at 2.752(3) Å, and a long Bi−Se bond at 3.125(3) Å trans to it. The coordination environments of Bi(2) and Bi(3) have the same characteristics. Bi(4) and Bi(5) exhibit a different kind of distortion having three short bonds trans to three longer ones. For example, Bi(4) has two short bonds at 2.766(2) Å, one slightly longer bond at 2.859(3) Å, and three longer bonds between 3.148(3) and 3.211(2) Å.

β-$RbBi_3Se_5$ exhibits the same characteristics with the only departure being the different occupancies of the alkali metal ions between the layers compared to the occupancies of the Cs analogue. Selected distances and angles are shown in Table 6.

D. γ-$RbBi_3Se_5$ (IV) and $RbBi_3Se_4Te$ (VI). These two compounds are isostructural; therefore, only γ-$RbBi_3Se_5$ will

Table 6. Bond Distances (Å) and Selected Angles (deg) for $CsBi_3Se_5$ and β-$RbBi_3Se_5$

$CsBi_3Se_5$		β-$RbBi_3Se_5$	
Bi(1)−Se(1)	2.752(3)	Bi(1)−Se(1)	2.740(3)
Bi(1)−Se(2)	2.941(2) × 2	Bi(1)−Se(2)	2.946(2) × 2
Bi(1)−Se(1)	2.980(2) × 2	Bi(1)−Se(1)	2.969(2) × 2
Bi(1)−Se(6)	3.125(3)	Bi(1)−Se(6)	3.134(2)
Bi(2)−Se(2)	2.797(3)	Bi(2)−Se(2)	2.776(3)
Bi(2)−Se(6)	2.939(2) × 2	Bi(2)−Se(6)	2.956(2) × 2
Bi(2)−Se(3)	2.982(2) × 2	Bi(2)−Se(3)	2.970(2) × 2
Bi(2)−Se(7)	3.117(2)	Bi(2)−Se(7)	3.136(2)
Bi(3)−Se(3)	2.768(3)	Bi(3)−Se(3)	2.750(2)
Bi(3)−Se(4)	2.899(2) × 2	Bi(3)−Se(4)	2.885(2) × 2
Bi(3)−Se(7)	3.017(2) × 2	Bi(3)−Se(7)	3.024(2) × 2
Bi(3)−Se(8)	3.194(3)	Bi(3)−Se(8)	3.190(2)
Bi(4)−Se(5)	2.766(2)	Bi(4)−Se(5)	2.773(2) × 2
Bi(4)−Se(4)	2.859(3)	Bi(4)−Se(4)	2.860(2)
Bi(4)−Se(9)	3.148(3)	Bi(4)−Se(9)	3.124(2)
Bi(4)−Se(8)	3.211(2) × 2	Bi(4)−Se(8)	3.194(2) × 2
Bi(5)−Se(10)	2.766(2) × 2	Bi(5)−Se(10)	2.775(2) × 2
Bi(5)−Se(6)	2.891(3)	Bi(5)−Se(6)	2.866(2)
Bi(5)−Se(9)	3.082(3)	Bi(5)−Se(9)	3.079(2)
Bi(5)−Se(7)	3.206(2) × 2	Bi(5)−Se(7)	3.184(2) × 2
Bi(6)−Se(9)	2.884(2) × 2	Bi(6)−Se(9)	2.881(2) × 2
Bi(6)−Se(8)	2.925(3)	Bi(6)−Se(8)	2.925(2)
Bi(6)−Se(7)	2.974(2)	Bi(6)−Se(7)	2.947(2)
Bi(6)−Se(8)	3.024(2) × 2	Bi(6)−Se(8)	3.032(2) × 2
Cs(1)−Se−(9-coordinate)	3.311(6)−4.072(5)	Rb(1)−Se−(9-coordinate)	3.24(1)−3.97(1)
Cs(2)−Se−(8-coordinate)	3.460(5)−4.068(6)	Rb(2)−Se−(8-coordinate)	3.45(2)−4.23(2)
Cs(3)−Se−(6-coordinate)	3.756(9)−4.02(1)	Rb(3)−Se−(6-coordinate)	3.71(1)−4.11(2)
Cs(4)−Se−(7-coordinate)	3.09(1)−3.93(1)	Rb(4)−Se−(7-coordinate)	3.26(2)−3.91(2)
Cs(5)−Se−(6-coordinate)	3.655(9)−3.845(8)	Rb(5)−Se−(6-coordinate)	3.65(1)−3.87(2)
Cs(6)−Se−(6-coordinate)	3.798(8)−4.01(1)	Rb(6)−Se−(6-coordinate)	3.74(2)−4.11(4)
Se(2)−Bi(1)−Se(6)	86.73(7)	Se(2)−Bi(1)−Se(6)	87.54(6)
Se(1)−Bi(1)−Se(2)	92.34(7)	Se(1)−Bi(1)−Se(2)	91.71(6)
Se(2)−Bi(1)−Se(1)	177.19(8)	Se(2)−Bi(1)−Se(1)	177.58(8)
Se(3)−Bi(2)−Se(7)	86.70(6)	Se(3)−Bi(2)−Se(7)	86.45(6)
Se(2)−Bi(2)−Se(6)	93.16(6)	Se(2)−Bi(2)−Se(6)	94.41(6)
Se(6)−Bi(2)−Se(3)	174.76(7)	Se(6)−Bi(2)−Se(3)	174.14(7)
Se(7)−Bi(3)−Se(8)	83.80(5)	Se(7)−Bi(3)−Se(8)	83.28(5)
Se(3)−Bi(3)−Se(4)	93.94(6)	Se(3)−Bi(3)−Se(4)	94.49(6)
Se(4)−Bi(3)−Se(7)	173.00(7)	Se(4)−Bi(3)−Se(7)	172.26(7)
Se(8)−Bi(4)−Se(8)	80.50(6)	Se(8)−Bi(4)−Se(8)	80.86(6)
Se(5)−Bi(4)−Se(5)	97.24(9)	Se(5)−Bi(4)−Se(5)	96.68(9)
Se(4)−Bi(4)−Se(9)	170.22(7)	Se(4)−Bi(4)−Se(9)	170.70(7)
Se(7)−Bi(5)−Se(7)	80.66(5)	Se(7)−Bi(5)−Se(7)	81.18(5)
Se(10)−Bi(5)−Se(10)	97.21(10)	Se(10)−Bi(5)−Se(10)	96.59(9)
Se(6)−Bi(5)−Se(9)	169.09(8)	Se(6)−Bi(5)−Se(9)	170.65(7)
Se(8)−Bi(6)−Se(8)	86.67(7)	Se(8)−Bi(6)−Se(8)	86.21(6)
Se(9)−Bi(6)−Se(8)	92.67(6)	Se(9)−Bi(6)−Se(8)	92.59(6)
Se(8)−Bi(6)−Se(7)	172.82(7)	Se(8)−Bi(6)−Se(7)	172.56(7)

be described in detail and then compared to $RbBi_3Se_4Te$. This structure is layered, and its slabs consist of Bi_2Te_3-type infinite rods fragments which are three Bi octahedra wide; see Figure 7a. It is interesting to compare this structure with that of $RbPbBi_3Se_6$[7] in which the layers are composed of complete Bi_2Te_3-type layers. $RbPbBi_3Se_6$ can be thought essentially as Bi_2Te_3 with alkali metals residing between the layers. By comparison, in γ-$RbBi_3Se_5$ these Bi_2Te_3-type fragments are sliced to three bismuth octahedra wide and rejoined in an offset manner creating stepwise corrugated layers; see Figure 7b. Adjacent layers are running in opposite directions creating a center of symmetry in the crystal. The Rb atoms reside in the space formed between the layers.

The three Bi sites have distorted octahedral coordination (Table 7). Bi(1) that connects the Bi_2Te_3-type blocks together is the least distorted with Bi(1)−Se bonds varying between 2.864(4) and 2.961(4) Å and Se−Bi(1)−Se angles varying between 88.58(14)° and 91.05(8)°. Bi(3) is distorted toward a trigonal pyramid with three short distances trans to three longer ones, while Bi(2) is distorted toward a square pyramid with one short bond at 2.773(3) Å, four bonds between 2.901(3) and 3.012(4) Å, and one long bond at 3.131(4) Å trans to the short bond. The Rb atoms have a bicapped trigonal prismatic coordination with Rb−Se distances varying between 3.413(6) and 3.796(6) Å.

Interestingly, in $RbBi_3Se_4Te$ the Te atoms are not statistically disordered, overall, in Se sites but seem to preferentially occupy two chalcogen sites that are on the surface of the layers. Both sites are occupied by ∼50% Te. Selected distances and angles are shown in Table 7. It is tempting to speculate that the lamellar

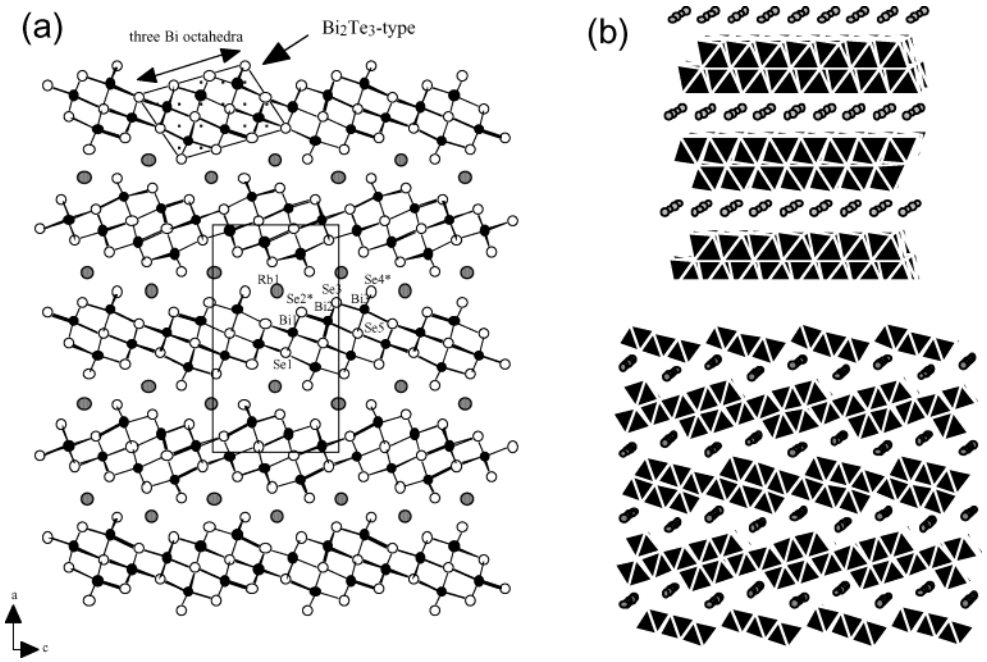

Figure 7. (a) Projection of the structure of γ-$RbBi_3Se_5$ (also adopted by $RbBi_3Se_4Te$) down the *b*-axis. The shaded area indicates the Bi_2Te_3-type building block, and the (*)'s indicate the Te containing chalcogen sites in $RbBi_3Se_4Te$. (b) Polyhedral representation of the structures of $RbPbBi_3Se_6$ (top) and γ-$RbBi_3Se_5$ (bottom).

Table 7. Bond Distances (Å) and Selected Angles (deg) for γ-$RbBi_3Se_5$ and $RbBi_3Se_4Te$

γ-$RbBi_3Se_5$		$RbBi_3Se_4Te$	
Bi(1)−Se(1)	2.864(4)	Bi(1)−Se(1)	2.859(4)
Bi(1)−Se(1)	2.942(3) × 2	Bi(1)−Se(1)	2.975(3) × 2
Bi(1)−Se(5)	2.955(5)	Bi(1)−Se(5)	3.035(4)
Bi(1)−Se(2)	2.961(4) × 2	Bi(1)−Q(2)[a]	3.076(2) × 2
Bi(2)−Se(2)	2.773(5)	Bi(2)−Q(2)	2.912(3)
Bi(2)−Se(3)	2.901(3) × 2	Bi(2)−Se(3)	2.951(2) × 2
Bi(2)−Se(5)	3.012(4) × 2	Bi(2)−Se(5)	3.018(3) × 2
Bi(2)−Se(5)	3.131(5)	Bi(2)−Se(5)	3.154(4)
Bi(3)−Se(4)	2.784(4) × 2	Bi(3)−Q(4)	2.918(2) × 2
Bi(3)−Se(3)	2.840(5)	Bi(3)−Se(3)	2.855(4)
Bi(3)−Se(1)	3.064(4)	Bi(3)−Se(1)	3.146(4)
Bi(3)−Se(5)	3.227(4) × 2	Bi(3)−Se(5)	3.240(3) × 2
Rb(1)−Se(1)	3.413(6)	Rb(1)−Se(1)	3.429(5)
Rb(1)−Se(4)	3.490(7)	Rb(1)−Q(4)	3.563(5)
Rb(1)−Se(3)	3.499(5) × 2	Rb(1)−Se(3)	3.519(4) × 2
Rb(1)−Se(2)	3.711(6) × 2	Rb(1)−Q(2)	3.803(4) × 2
Rb(1)−Se(4)	3.796(6) × 2	Rb(1)−Q(4)	3.783(4) × 2
Se(2)−Bi(1)−Se(2)	88.6(1)	Q(2)−Bi(1)−Q(2)	86.66(9)
Se(1)−Bi(1)−Se(2)	91.05(8)	Se(1)−Bi(1)−Q(2)	91.62(8)
Se(1)−Bi(1)−Se(5)	178.9(1)	Se(1)−Bi(1)−Se(5)	177.8(1)
Se(5)−Bi(2)−Se(5)	83.5(1)	Se(5)−Bi(2)−Se(5)	88.8(1)
Se(2)−Bi(2)−Se(5)	92.8(1)	Q(2)−Bi(2)−Se(5)	93.54(9)
Se(3)−Bi(2)−Se(5)	173.0(1)	Se(3)−Bi(2)−Se(5)	174.6(1)
Se(5)−Bi(3)−Se(5)	79.7(1)	Se(5)−Bi(3)−Se(5)	81.32(8)
Se(4)−Bi(3)−Se(4)	95.9(2)	Q(4)−Bi(3)−Q(4)	92.7(1)
Se(3)−Bi(3)−Se(1)	168.1(1)	Se(3)−Bi(3)−Se(1)	168.5(1)

[a] Q = Se and Te.

structure of the γ-form is adopted in this case because the larger tellurium atoms need more space to be accommodated. A three-dimensional framework (i.e., that of the α-form) may not have much room to expand, upon replacement of Se with Te atoms, and at the same time achieve optimum packing. By placing the Te atoms on the "surface" of the $[Bi_3Q_5]$ slab, some of the lattice expansion can be conveniently achieved by increasing the interlayer distance (i.e., *a*-axis). It is not clear yet why a compound with the formula $RbBi_3(Se,Te)_5$ adopting the β-structure type is not observed.

Comparison of the AM_3Q_5 Structures. It is remarkable and extraordinary that the general formula AM_3Q_5 where M is an octahedrally bonded metal atom and Q is a chalcogen atom generates more than seven structural motifs. It is also exceptional that with the same element, that is, Bi, at least five different designs are observed. Although extensive variation in crystal structure is observed in certain materials exhibiting polytypism, for example, SiC, CdI_2, and so forth, the polytypes are closely related in structure and differ only by simple displacements or changes in stacking sequence. This is not the case with the AM_3Q_5 phases where each structure type has a distinct architecture.

The three polymorphic versions of $RbBi_3Se_5$ have different asymmetric units. In the γ-form the asymmetric unit has the formula "*$RbBi_3Se_5$*", in the β-form has the formula "*$Rb_2Bi_6Se_{10}$*" and in the α-form "*$Rb_3Bi_9Se_{15}$*". The compounds can be regarded as members of a homologous series $(ABi_3Se_5)_n$, where $n = 1, 2, 3...$ As the formula of the asymmetric unit increases, we have a gradual increase in the complexity of the structure. γ-$RbBi_3Se_5$ with $n = 1$ contains only simple three octahedra-wide Bi_2Te_3-type fragments. β-$RbBi_3Se_5$, on the other hand, although also made of one block (NaCl-type), is more elaborate. α-$RbBi_3Se_5$, in turn, is made up of two different building blocks (Bi_2Te_3- and CdI_2-type, two different sets of each block). This increase in structural complexity among polymorphs is an exceptional example in the bismuth chalcogenide family.

When the densities are examined, α-$RbBi_3Se_5$ is the most dense ($d = 6.611$ g/cm^3) followed by γ-$RbBi_3Se_5$ ($d = 6.555$ g/cm^3) and β-$RbBi_3Se_5$ ($d = 6.088$ g/cm^3). β-$RbBi_3Se_5$ is the least dense compound because it contains a great number of partially occupied Rb sites. If we compare the volumes of α- and γ-$RbBi_3S_5$ and KBi_3S_5 (β-$RbBi_3S_5$ has the same

Table 8. Unit Cell Parameters and Volumes for Several AM_3Q_5 Structures

formula	*a* (Å)	*b* (Å)	*c* (Å)	β (deg)	volume (Å^3)	space group	reference
α-$RbBi_3S_5$	4.16(1)	12.90(2)	18.47(8)	90	987.7	*Pmnn* (#58)	15f
γ-$RbBi_3S_5$	11.744(2)	4.0519(5)	21.081(3)	90	1003.1(2)	*Pnma* (#62)	*a*
$CsBi_3S_5$	4.064(1)	12.098(3)	21.098(4)	90	1037.4	*Pmnb* (#62)	15e
α-$RbBi_3Se_5$	36.779(4)	4.1480(5)	25.363(3)	120.403(2)	3337.3(7)	*C2/m* (#12)	*a*
β −$RbBi_3Se_5$	13.537(2)	4.1431(6)	21.545(3)	91.297(3)	1208.0(3)	$P2_1/m$ (#14)	*a*
$CsBi_3Se_5$	13.603(3)	4.1502(8)	21.639(4)	92.453(3)	1221.2(4)	$P2_1/m$ (#14)	*a*
γ-$RbBi_3Se_5$	21.956(7)	4.136(1)	12.357(4)	90	1122.0(6)	*Pnma* (#62)	*a*
$RbBi_3Se_4Te$	22.018(3)	4.2217(6)	12.614(2)	90	1172.5(3)	*Pnma* (#62)	*a*
KBi_3S_5[b]	17.013(5)	4.076(2)	17.365(4)	90	1122.0(6)	*Pnma* (#62)	2
$CsEr_3Se_5$	22.059(9)	4.095(2)	12.155(5)	90	1098.0	*Pnma* (#62)	30
$TlIn_3S_5$[c]	20.258(6)	3.826(1)	12.821(3)	121.4	848.3	*C2/m* (#12)	31

[a] This work. [b] β-$RbBi_3S_5$ has the structure of KBi_3S_5 (ion exchange product). [c] Other compounds such as ACr_3S_5 (A= Rb, Tl) adopt the same structure type.

structure as KBi_3S_5), we notice that the α-form is more dense with the smallest volume followed by the γ-form. KBi_3S_5 is the least dense because of its unusually open framework structure.[2]

Several other chalcogenides with the formula AM_3Q_5 [29] have similar unit cells and cell volumes to the compounds described here; see Table 8. Yet most of these compounds adopt different structure types albeit the building blocks involved are similar. Most compounds in the AM_3Q_5 class consist only of one type of building block. For example, KBi_3S_5,[2] $CsEr_3Se_5$, [30] and $TlIn_3S_5$ [31] are made only of CdI_2-type fragments, whereas α-$RbBi_3S_5$ [15f] has only NaCl-type blocks; see Figures 4 and 8. KBi_3S_5, $CsEr_3Se_5$, and $TlIn_3S_5$ are open framework tunnel structures with CdI_2-type blocks running in two different directions. This is a characteristic that is also found in α-$RbBi_3Se_5$. The size, shape, and "packing" of the tunnels vary from structure to structure. In KBi_3S_5, the tunnels are 5×4 octahedra large and can accommodate four potassium sites (partially occupied), while, in $CsEr_3Se_5$ and $TlIn_3S_5$, the tunnels still have the same dimensions but accommodate two fully occupied sites. The difference between the last two structures is the different packing of these tunnels. In $CsEr_3Se_5$, these tunnels are arranged in a zigzag fashion while in, $TlIn_3S_5$, the tunnels are parallel with each other. These phases are expected to exhibit good ion-exchange properties. In α-$RbBi_3Se_5$, the size of the tunnels is considerably larger (6×7 octahedra) than those found in the other compounds.

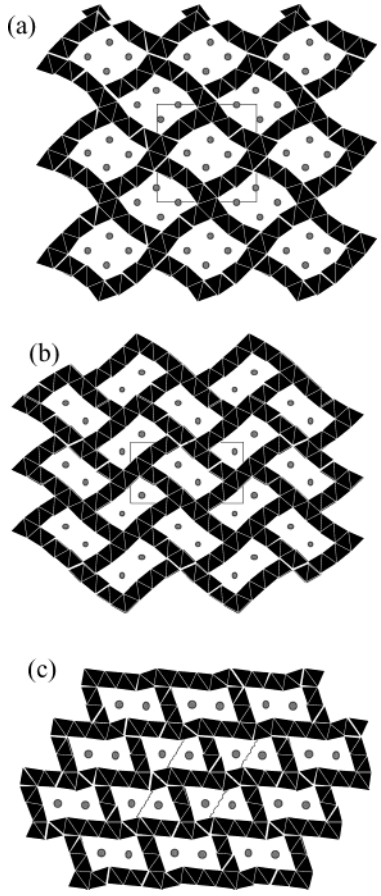

Figure 8. Comparative view of the structures of (a) KBi_3S_5, (b) $CsEr_3Se_5$, and (c) $TlIn_3S_5$ down the *b*-axis.

Concluding Remarks

The existence of the phases described here demonstrates a remarkable variety and sophistication found in all the bismuth chalcogenides systems. The six compounds with the general formula ABi_3Q_5 (A = Rb, Cs; Q = S, Se, Te) exhibit considerable polymorphism. Very few other chemical systems are capable of exhibiting the ability to adopt alternate structural arrangements (for a given composition) as a response to relatively small changes in experimental conditions. The γ-$RbBi_3S_5$ and $RbBi_3Se_4Te$ melt congruently, whereas α-, β-, and γ-$RbBi_3Se_5$ and $CsBi_3Se_5$ transform to $Rb_2Bi_8Se_{13}$ and $CsBi_{3.67}Se_6$, respectively. γ-$RbBi_3Se_5$ seems to be the most stable form, and this is supported also by DFT band structure calculations. The AM_3Q_5 (Q = S, Se) composition is very common among alkali metal chalcogenides when the metal has both a +3 formal oxidation state and an octahedral coordination preference. It is remarkable however that when M = Bi, approximately ten different compounds are possible adopting six different structure types.[32] Although the various chemical reasons and characteristics discussed in the Introduction can justify the plethora of compositions and structural types encountered in bismuth chalcogenides, they cannot predict or account for the occurrence of polymorphs. The latter are more common in simpler systems as elemental structures and binary phases. This implies that additional and more subtle factors

(29) We searched the ICSD database for compounds with the general formula AB_3Q_5 where Q = chalcogenide that have a similar unit cell, a similar cell volume, or similar building blocks with the compounds presented in this paper. Compounds that had the same general formula but did not possess any similarity were not included in the comparison.

(30) Kim, S.-J.; Park, S.-J.; Yun H.; Do, J. *Inorg. Chem.* **1996**, *35*, 5283−5289.
(31) Walther, R.; Deiseroth, H. J. *Z. Kristallogr.* **1996**, *211*, 49.

(32) Including the questionable α-$RbBi_3S_5$.

operate in these systems that are yet to be recognized and enumerated. As a set, the compounds of ABi_3Q_5 present a complete series of varying structures that possess enough complexity to stimulate new theoretical studies aimed at understanding the relationships and interplay of packing factors vis a vis electronic factors in dictating crystal structure.

Acknowledgment. Financial support from the Office of Naval Research (Contract No. N00014-02-1-0867) is gratefully acknowledged. The work made use of the SEM facilities of the Center for Advanced Microscopy at Michigan State University.

Supporting Information Available: X-ray crystallographic data (for compounds I, II, III, IV, V, and VI). This material is available free of charge via the Internet at http://pubs.acs.org.

JA034196P